AD-A091 893 PROPELLANTS EXPLOSIVES AND ROCKET MOTOR ESTABLISHMENT--ETC F/G 21/2
PRODUCTION OF NITROUS OXIDE IN A ROCKET MOTOR EXHAUST.(U)
AUG 80 D E JENSEN
UNCLASSIFIED PERME-MEMO-96 DRIC-BR-75265 NL

END
DATE
FILMED
1-81
DTIC

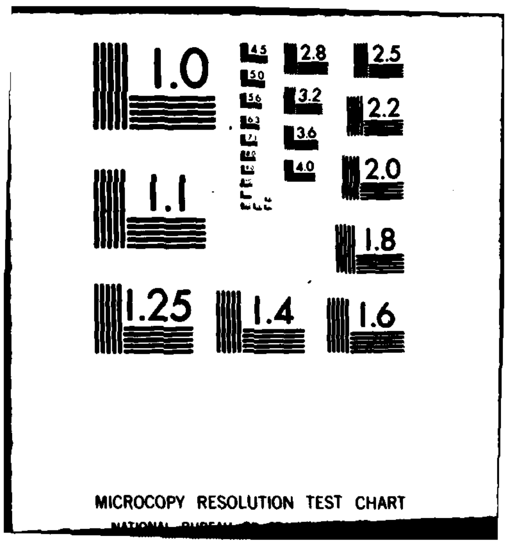
1.0
4.5
5.0
5.6
6.3
2.8
3.2
3.6
4.0
2.5
2.2
2.0
1.1
1.8
1.25
1.4
1.6
MICROCOPY RESOLUTION TEST CHART

UNLIMITED

PROPELLANTS, EXPLOSIVES AND ROCKET MOTOR ESTABLISHMENT
WESTCOTT

Memorandum No. 96

Approved December 1979

PRODUCTION OF NITROUS OXIDE IN A ROCKET MOTOR EXHAUST

by

D.E. Jensen

10 to the 12th power and 10 to the 13th power molecule/ml,

SUMMARY

Predictions are made of concentrations of N_2O produced within the exhaust of a double-base propellant rocket motor. Typical concentrations produced are predicted to be between 10^{12} and 10^{13} molecule ml^{-1}, some five orders of magnitude below those of CO_2 and lower than the characteristic atmospheric level of about 1.3×10^{13} molecule ml^{-1}.

1.3 X 10 to the 13th power molecule/ml.

1 INTRODUCTION

Emissions in the carbon dioxide $\Sigma_u^+ (0, 0^0, 1) - \Sigma_g^+ (0, 0^0, 0)$ band and other, overlapping, CO_2 bands at wavelengths ≈ 4.3 μm are a prominent infrared feature of rocket exhaust flames. Nitrous oxide $\Sigma^+ (0, 0, 1) - \Sigma^+ (0, 0, 0)$ band emissions also occur at these wavelengths, and absorption of both N_2O and CO_2 radiations results from the presence of these molecules in the atmosphere. Atmospheric concentrations of CO_2 and N_2O are approximately 8×10^{15} and 1.3×10^{13} molecule ml^{-1} respectively[1], and rocket exhaust CO_2 concentrations may be calculated with satisfactory accuracy by the methods of Ref. 2 and 3. Exhaust concentrations of N_2O have not previously been calculated, however. This memorandum summarizes results of a calculation of N_2O production in a particular exhaust.

2 METHOD OF CALCULATION

Calculation of a rocket exhaust structure (the distribution in space of temperature, species concentrations, etc.) proceeds in three stages. First, conditions in the chamber are calculated[4] on the basis of the assumption that chemical equilibrium is achieved at the high temperatures and pressures encountered therein. Secondly, the nozzle flow is treated by a method which allows for non-equilibrium chemical effects (a simplified one-dimensional treatment[4] was used in the present work), and the nozzle exit conditions are obtained. Thirdly, the exhaust structure is computed from knowledge of these exit conditions and such external quantities as missile velocity and altitude.

The third stage of the calculation is the most difficult. The technique used here[2,3,5] stems from coupling together a two-equation model of turbulence[6] and detailed non-equilibrium chemistry. The two turbulence variables for which equations were solved in this work were the turbulence kinetic energy k (half the sum of the squares of RMS fluctuating parts of velocity components) and W, the square of a frequency characteristic of the energy-containing eddies.

The governing equations, assumptions, boundary conditions and method of finite-difference solution are indicated elsewhere[2,3,5]. With the notation of Ref. 2,

the turbulence model constants used here took the following values: $C_1 = 3.5$, $C_2 = 0.17$, $C_3 = 1.48$, $C_D = 0.09$; turbulent Prandtl and Schmidt numbers Pr_t and $Sc_t = 1.0$, corresponding coefficients for k and $W = 0.86$. No equation was included here for the g variable of Ref. 2. The set of reversible chemical reactions (with rate coefficients) used for the exhaust calculation is shown in Table 1. Reactions 1-18 constitute a basic exhaust combustion mechanism (cf. Ref. 5). Reactions 19-34 are designed to account for production of N_2O, both directly from N_2, O_2 and O and indirectly via NO, HNO, N and NO_2. Rate coefficients for reactions 1-25 are taken from Ref. 7; those for reactions 26-34 derive directly from Ref. 8. Thermochemical data for all species stem from Ref. 9. The same set of chemical data was used for the nozzle calculation. The species PbO, SnO and Ca were treated, for the present purpose, as chemically inert, PbO and SnO being assumed to be present as solid particles small enough to follow gas streamlines.

Exit conditions for the selected (double-base solid propellant) rocket motor are shown in Table 2. The calculation was performed for static sea-level conditions, with an atmosphere temperature and pressure of 288 K and 1.013×10^5 N m^{-2} respectively and an atmospheric composition of $[N_2] = 2.02 \times 10^{19}$, $[O_2] = 5.31 \times 10^{18}$, $[CO_2] = 8.38 \times 10^{15}$ and [other species] = 0 molecule ml^{-1}. (No N_2O was included in the atmospheric composition for the calculation because interest was centered on production of this species in the exhaust rather than its entrainment from the atmosphere.) The exhaust was axisymmetric and contained no significant region of base recirculation.

3 RESULTS

Selected outputs from the calculation are shown in Figs. 1-5. Fig. 1 shows variations of $[N_2O]$ with radial distance r from the exhaust axis for specified axial distances x downstream of the nozzle exit. Peak concentrations of N_2O are $\approx 3 \times 10^{12}$ molecule ml^{-1}, with an uncertainty factor probably of about 3. Corresponding radial temperature profiles appear in Fig. 2. Radial profiles of $[CO_2]$ at

TABLE I

Reaction mechanism for N_2O calculations

	Reaction	Rate Coefficient[a]
1	$O + O + M \rightarrow O_2 + M$	$3 \times 10^{-34}\ \exp(900/T)$
2	$O + H + M \rightarrow OH + M$	$1 \times 10^{-29}\ T^{-1}$
3	$H + H + M \rightarrow H_2 + M$	$3 \times 10^{-30}\ T^{-1}$
4	$H + OH + M \rightarrow H_2O + M$	$1 \times 10^{-25}\ T^{-2}$
5	$CO + O + M \rightarrow CO_2 + M$	$7 \times 10^{-33}\ \exp(-2200/T)$
6	$OH + H_2 \rightarrow H_2O + H$	$1.9 \times 10^{-15}\ T^{1.3}\ \exp(-1825/T)$
7	$O + H_2 \rightarrow OH + H$	$3 \times 10^{-14}\ T\ \exp(-4480/T)$
8	$H + O_2 \rightarrow OH + O$	$2.4 \times 10^{-10}\ \exp(-8250/T)$
9	$CO + OH \rightarrow CO_2 + H$	$2.8 \times 10^{-17}\ T^{1.3}\ \exp(330/T)$
10	$OH + OH \rightarrow H_2O + O$	$1 \times 10^{-11}\ \exp(-550/T)$
11	$CO + O_2 \rightarrow CO_2 + O$	$4.2 \times 10^{-12}\ \exp(-24000/T)$
12	$H + O_2 + M \rightarrow HO_2 + M$	$2 \times 10^{-32}\ \exp(500/T)$
13	$H + HO_2 \rightarrow OH + OH$	$4 \times 10^{-10}\ \exp(-950/T)$
14	$H + HO_2 \rightarrow H_2 + O_2$	$4 \times 10^{-11}\ \exp(-350/T)$
15	$H_2 + HO_2 \rightarrow H_2O + OH$	$1 \times 10^{-12}\ \exp(-9400/T)$
16	$CO + HO_2 \rightarrow CO_2 + OH$	$2.5 \times 10^{-10}\ \exp(-11900/T)$
17	$O + HO_2 \rightarrow OH + O_2$	$8 \times 10^{-11}\ \exp(-500/T)$
18	$OH + HO_2 \rightarrow O_2 + H_2O$	5×10^{-11}
19	$NO + NO \rightarrow N_2O + O$	$2.2 \times 10^{-12}\ \exp(-32100/T)$
20	$N_2O + H \rightarrow N_2 + OH$	$1.3 \times 10^{-10}\ \exp(-7600/T)$
21	$NO + H + M \rightarrow HNO + M$	$5 \times 10^{-32}\ \exp(300/T)$
22	$HNO + H \rightarrow NO + H_2$	8×10^{-12}
23	$HNO + OH \rightarrow NO + H_2O$	6×10^{-11}
24	$N_2 + O \rightarrow NO + N$	$1.3 \times 10^{-10}\ \exp(-38000/T)$
25	$N + O_2 \rightarrow NO + O$	$1.1 \times 10^{-14}\ T\ \exp(-3150/T)$
26	$N_2 + O_2 \rightarrow N_2O + O$	$1.1 \times 10^{-10}\ \exp(-55300/T)$
27	$N_2 + O + M \rightarrow N_2O + M$	$4 \times 10^{-35}\ \exp(-10660/T)$
28	$NO_2 + O \rightarrow NO + O_2$	$1.7 \times 10^{-11}\ \exp(-300/T)$
29	$NO_2 + H \rightarrow NO + OH$	$5.8 \times 10^{-10}\ \exp(-740/T)$
30	$N + N + M \rightarrow N_2 + M$	$8.3 \times 10^{-34}\ \exp(500/T)$
31	$N + O + M \rightarrow NO + M$	$1.8 \times 10^{-31}\ T^{-0.5}$
32	$NO + O + M \rightarrow NO_2 + M$	$3 \times 10^{-33}\ \exp(940/T)$
33	$N + OH \rightarrow NO + H$	7×10^{-11}
34	$HNO + HNO \rightarrow N_2O + H_2O$	$1 \times 10^{-12}\ \exp(-2000/T)$

TABLE 2

Rocket Motor Exit Plane Conditions

Quantity and Units		Value
Species concentration, molecule ml^{-1}:		
	CO_2	2.2×10^{18}
	N_2	1.8×10^{18}
	H_2O	3.3×10^{18}
	CO	4.7×10^{18}
	H_2	1.4×10^{18}
	H	8.7×10^{15}
	OH	4.7×10^{14}
	O_2	7.0×10^{12}
	O	2.4×10^{12}
	HO_2	9.3×10^{9}
	N_2O	9.4×10^{9}
	N	4.3×10^{9}
	NO	9.1×10^{14}
	NO_2	8.0×10^{7}
	HNO	2.6×10^{13}
	PbO	3.3×10^{16}
	SnO	1.8×10^{16}
	Ca	5.0×10^{15}
Jet velocity, km s^{-1}		2.2
Pressure, N m^{-2}		2.7×10^{5}
Temperature, K		1470
Nozzle radius, cm		5.74
Turbulence kinetic energy k, m^2 s^{-2}		7×10^{4}
W, s^{-2}		2.1×10^{9}
Mass flow rate, kg s^{-1}		13.3

the same axial stations are given in Fig. 3; comparison between Fig. 1 and Fig. 3 reveals that $[CO_2]$ typically exceeds $[N_2O]$ by about five orders of magnitude in the hotter parts of the exhaust. Axial profiles of $[N_2O]$ and temperature are shown in Figs. 4 and 5 respectively: both the shock structure close to the nozzle exit and the boost in temperature resulting from secondary combustion of CO and H_2 are clearly apparent.

Two subsidiary computations were performed. In the first, the sensitivity of results to Pr_t and Sc_t was illustrated via setting of these numbers to 0.7 rather than 1.0, all other inputs remaining unchanged. The distribution of temperature (Fig. 5) and of $[N_2O]$ (Fig. 6; compare Fig. 1) were not greatly affected, although the exhaust plume became slightly shorter and narrower. In the second, values of 0.7 for Pr_t and Sc_t were retained but all chemical reactions of nitrogen-containing species except 26 and 27 were omitted. This change, designed to isolate effects on $[N_2O]$ of two reactions regarded at the outset as likely to play dominant direct roles in determining this concentration, caused the predicted maximum concentration to rise by a factor of 2-3 (Fig. 7). Reactions other than 26 and 27 evidently do play significant parts in determining $[N_2O]$.

It is worth emphasising that N_2O concentrations produced in the exhaust are well away from those consistent with local thermochemical equilibrium. The last three columns of Table 3 show: (a) concentrations $[N_2O]_{27}$ calculated on the assumption that reaction 27 is locally balanced; (b) concentrations $[N_2O]_{26}$ calculated on the assumption that reaction 26 is locally balanced; and (c) concentrations $[N_2O]$ derived from the (standard inputs) exhaust structure calculation. $[N_2O]$ differs markedly from both $[N_2O]_{27}$ and $[N_2O]_{26}$ because non-equilibrium effects (especially those affecting $[O]$) are critically important.

TABLE 3

Non-equilibrium of N_2O-forming reactions

r, m	T, K	$[O]$	$[N_2]$	$[O_2]$	K_{27}	K_{26}	$[N_2O]_{27}$	$[N_2O]_{26}$	$[N_2O]$
0	2330	2.4×10^{15}	1.9×10^{18}	1.6×10^{17}	1.3×10^{-22}	1.4×10^{-8}	5.5×10^{11}	1.8×10^{12}	9.1×10^{11}
0.196	1750	5.2×10^{15}	2.8×10^{18}	4.6×10^{17}	1.7×10^{-21}	4.0×10^{-11}	2.5×10^{13}	9.7×10^{9}	1.9×10^{12}
0.327	1280	4.8×10^{14}	4.1×10^{18}	8.5×10^{17}	8.0×10^{-20}	7.0×10^{-15}	1.6×10^{14}	5.1×10^{7}	1.9×10^{12}
0.400	1040	7.1×10^{13}	5.2×10^{18}	1.2×10^{18}	2.2×10^{-18}	4.2×10^{-18}	8.1×10^{14}	3.5×10^{5}	1.6×10^{12}

Species concentrations in molecule ml^{-1}.

K_{27} and K_{26} are the equilibrium constants of reactions 27 and 26 respectively at the local temperatures.

$[N_2O]_{27}$ is calculated from $K_{27}\,[N_2][O]$ (i.e. on the assumption that reaction 27 is balanced).

$[N_2O]_{26}$ is calculated from $K_{26}\,[N_2][O_2]/[O]$.

$[N_2]$, $[O_2]$, $[O]$ and $[N_2O]$ are calculated with the input data and method of Section 2.

$x = 6.0$ m.

4 DISCUSSION AND CONCLUSIONS

The maximum concentration of N_2O produced in this exhaust is $\approx 3 \times 10^{12}$ molecule ml^{-1}. This is lower than the level of 1.3×10^{13} molecule ml^{-1} characteristically present on the atmosphere. The exhaust N_2O concentrations, even if raised somewhat via allowance for entrainment of atmospheric N_2O, are some five orders of magnitude below those of CO_2. It is likely that the main effect of N_2O on IR radiations at wavelengths $\approx$ 4.3 μm will be to cause atmospheric attenuation effects over long path lengths at certain specific wavelengths rather than to produce significant contributions to (exhaust) source radiation. Such a conclusion may reasonably be expected to hold for a wide range of rocket motors.

5 REFERENCES

No.	Author	Title, etc.
1	Anon	US Standard Atmosphere, 1962. NASA, USAF and United States Weather Bureau, 1962.
2	Jensen, D.E. Wilson, A.S.	Prediction of Rocket Exhaust Flame Properties. Combustion and Flame 1975, 25, 43
3	Jensen, D.E. Spalding, D.B. Tatchell, D.G. Wilson, A.S.	Computation of Structures of Flames with Recirculating Flow and Radial Pressure Gradients. Combustion and Flame 1979, 34, 309
4	Wilson, A.S.	A User's Guide to Computer Programs for the Calculation of Conditions in Flames and Rocket Nozzles. RPE Tech. Report No. 72/10 (1972)
5	Jensen, D.E. Jones, G.A.	Theoretical Aspects of Secondary Combustion in Rocket Exhausts. To be published.

No.	Author	Title, etc.
6	Launder, B.E.	Mathematical Models of Turbulence.
	Spalding, D.B.	Academic Press, London and New York, 1972
7	Jensen, D.E.	Reaction Rate Coefficients for Flame Calculations.
	Jones, G.A.	Combustion and Flame 1978, 32, 1
8	Baulch, D.L.	Evaluated Kinetic Data for High Temperature Reactions.
	Drysdale, D.D.	Vol. 2.
	Horne, D.G.	Butterworths, London, 1972.
	Lloyd, A.C.	
9	Stull, D.R.	JANAF Thermochemical Tables.
	Prophet, H.	NBS-NSRDS No. 37, 1971
		Supplement 1 : J. Phys. Chem. Ref. Data 1974, 3, 311
		Supplement 2 : J. Phys. Chem. Ref. Data 1975, 4, 1
		Supplement 3 : J. Phys. Chem. Ref. Data 1978, 7, 793

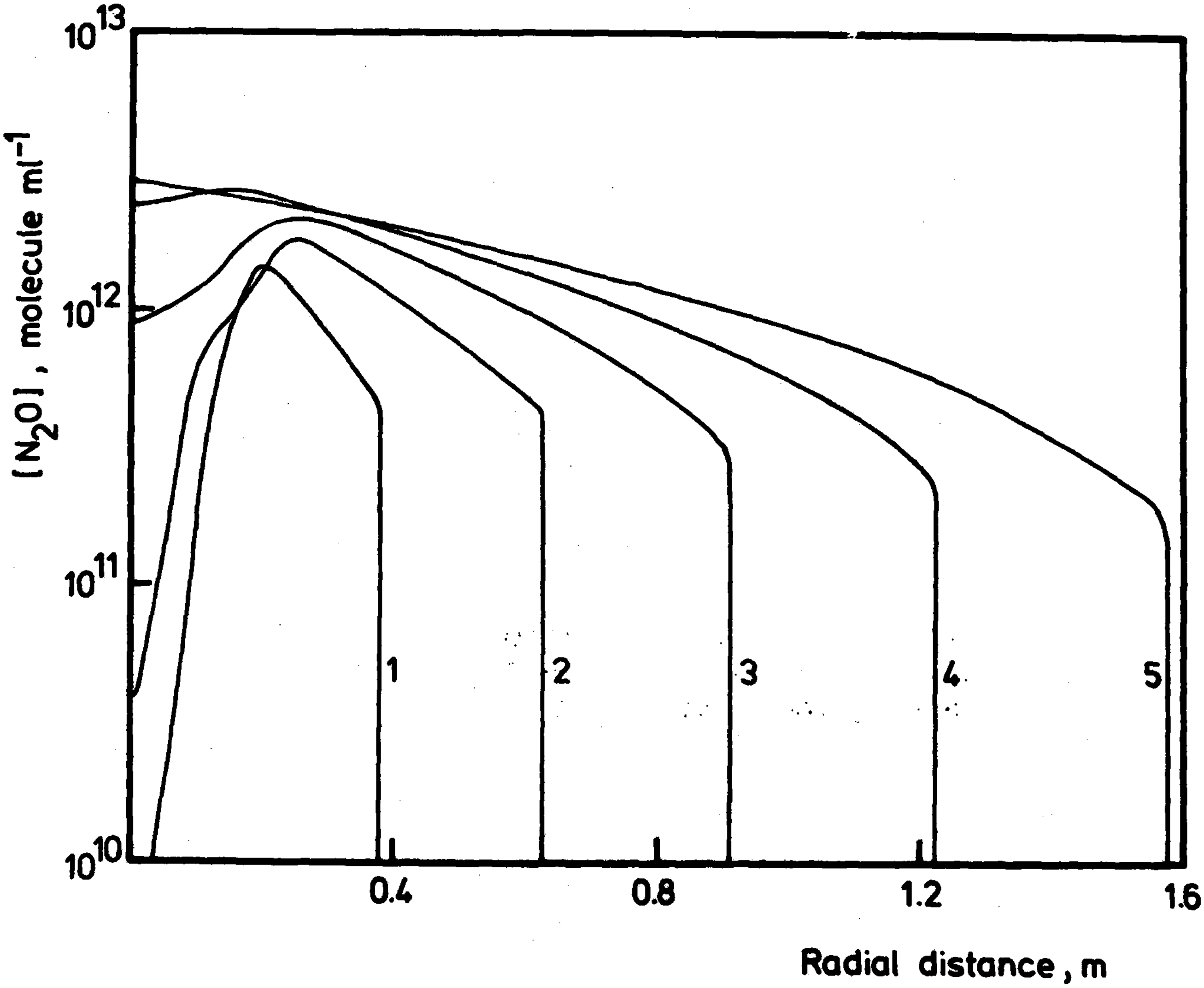

FIG. 1 RADIAL PROFILES OF $[N_2O]$ FOR CALCULATION WITH STANDARD INPUT DATA OF SECTION 2.

1, x = 2 m; 2, x = 4 m; 3, x = 6 m; 4, x = 8 m; 5, x = 10 m.

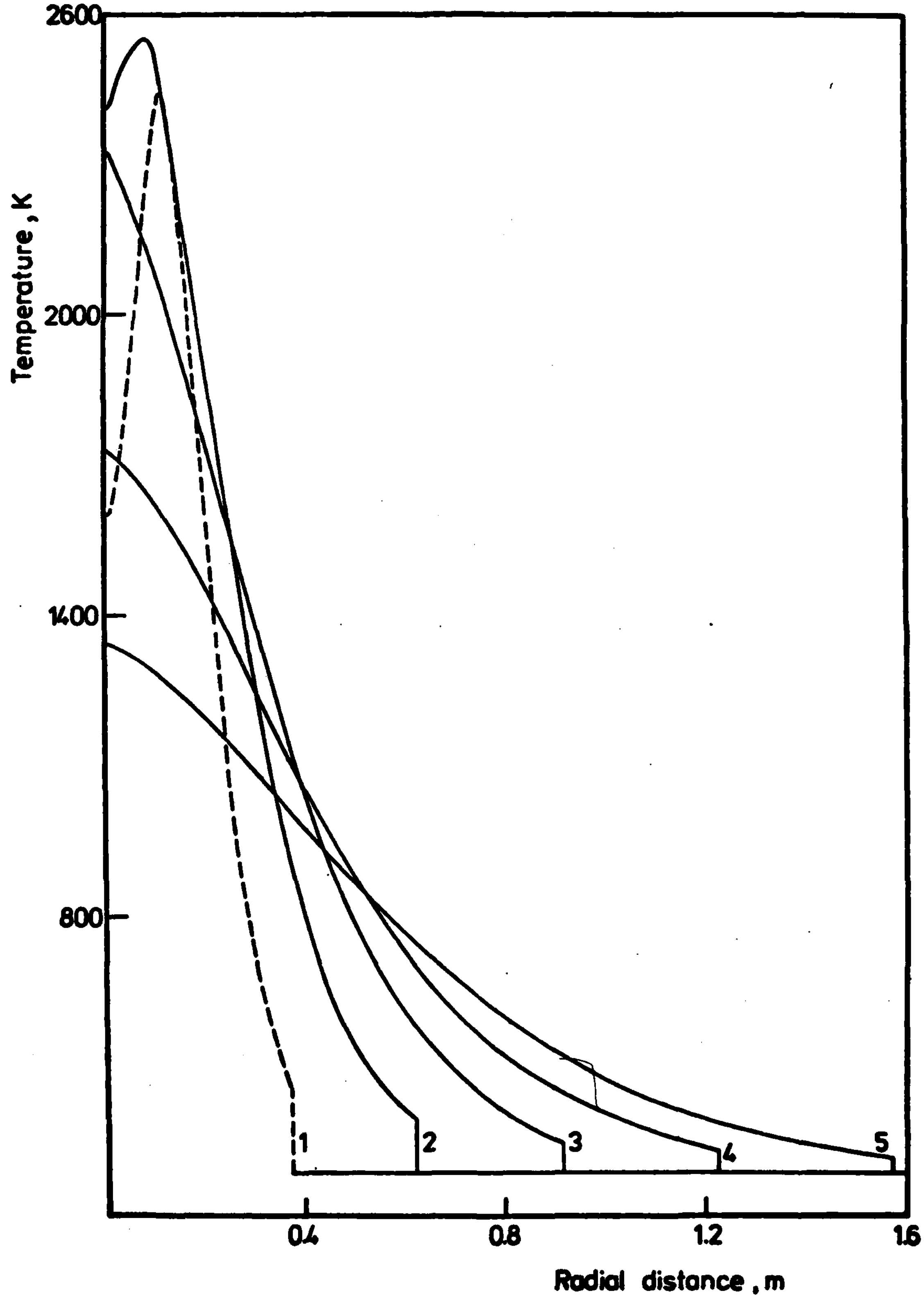

FIG. 2 RADIAL PROFILES OF TEMPERATURE FOR CALCULATION WITH STANDARD INPUT DATA OF SECTION 2.

1, x = 2 m; 2, x = 4 m; 3, x = 6 m; 4, x = 8 m; 5, x = 10 m.

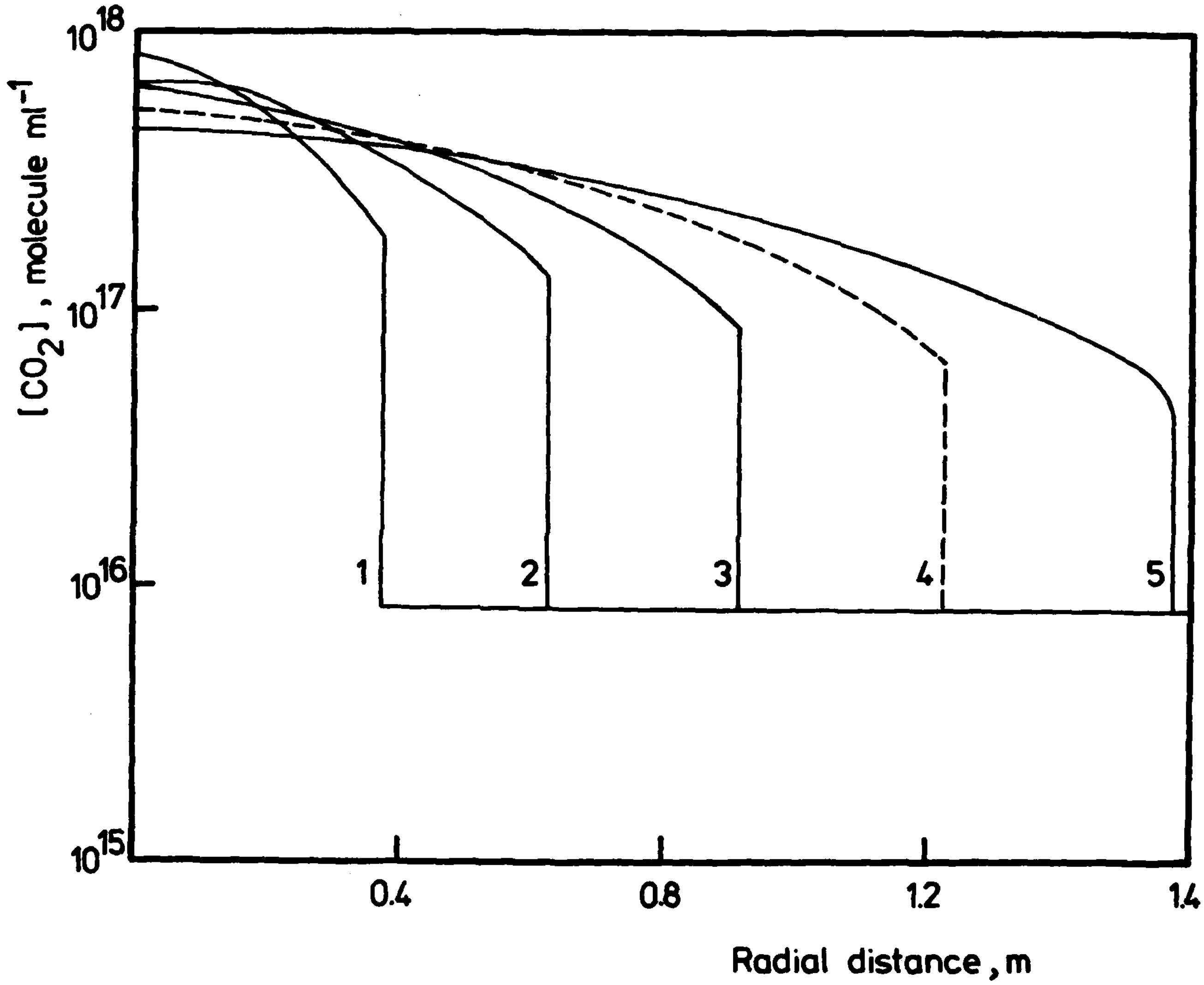

FIG. 3 RADIAL PROFILES OF $[CO_2]$ FOR CALCULATION WITH STANDARD INPUT DATA OF SECTION 2.

1, x = 2 m; 2, x = 4 m; 3, x = 6 m; 4, x = 8 m; 5, x = 10 m.

MEMO 96
FIG. 4

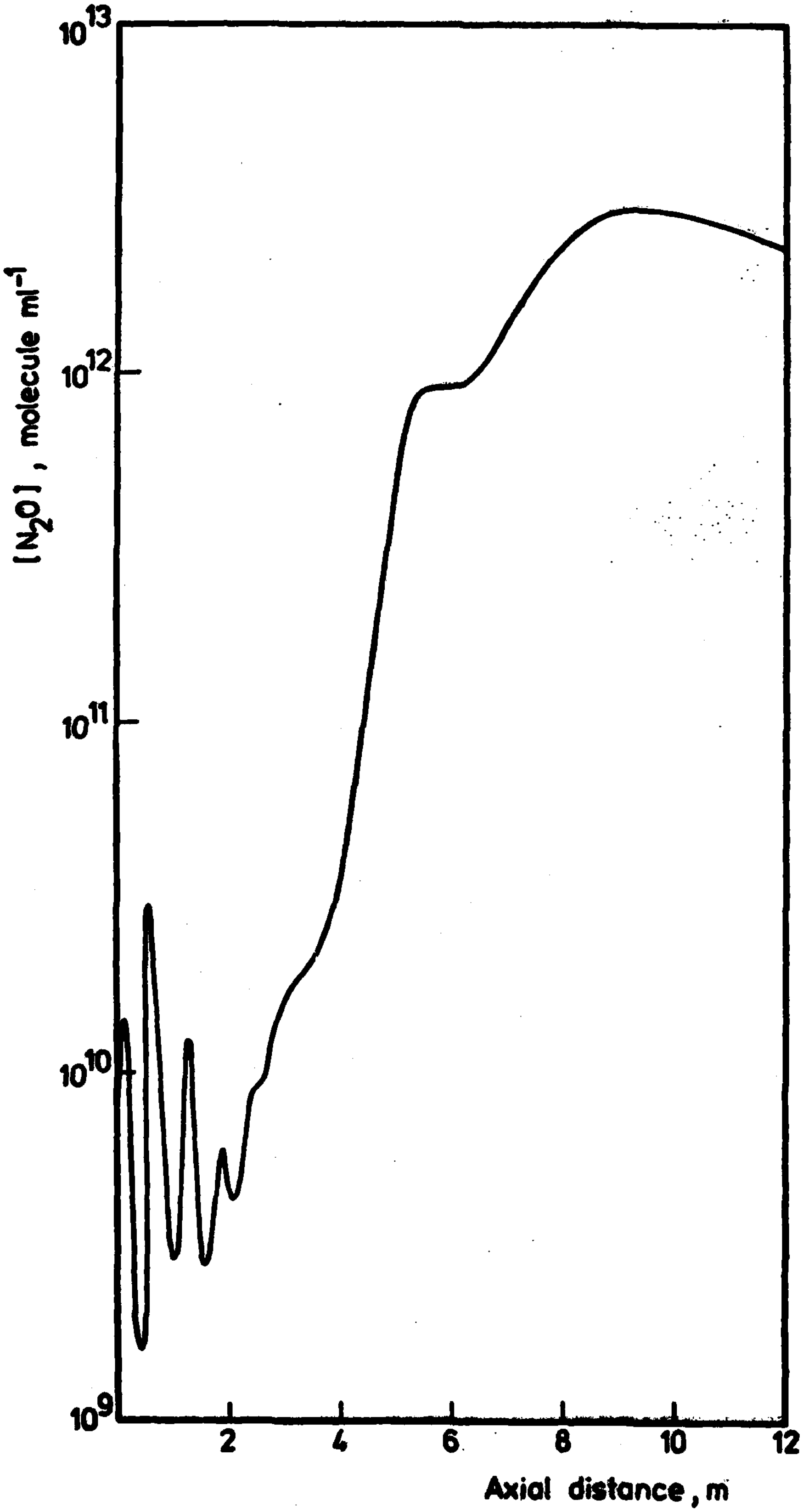

FIG. 4 AXIAL PROFILE OF $[N_2O]$ FOR CALCULATION WITH STANDARD INPUT DATA OF SECTION 2.

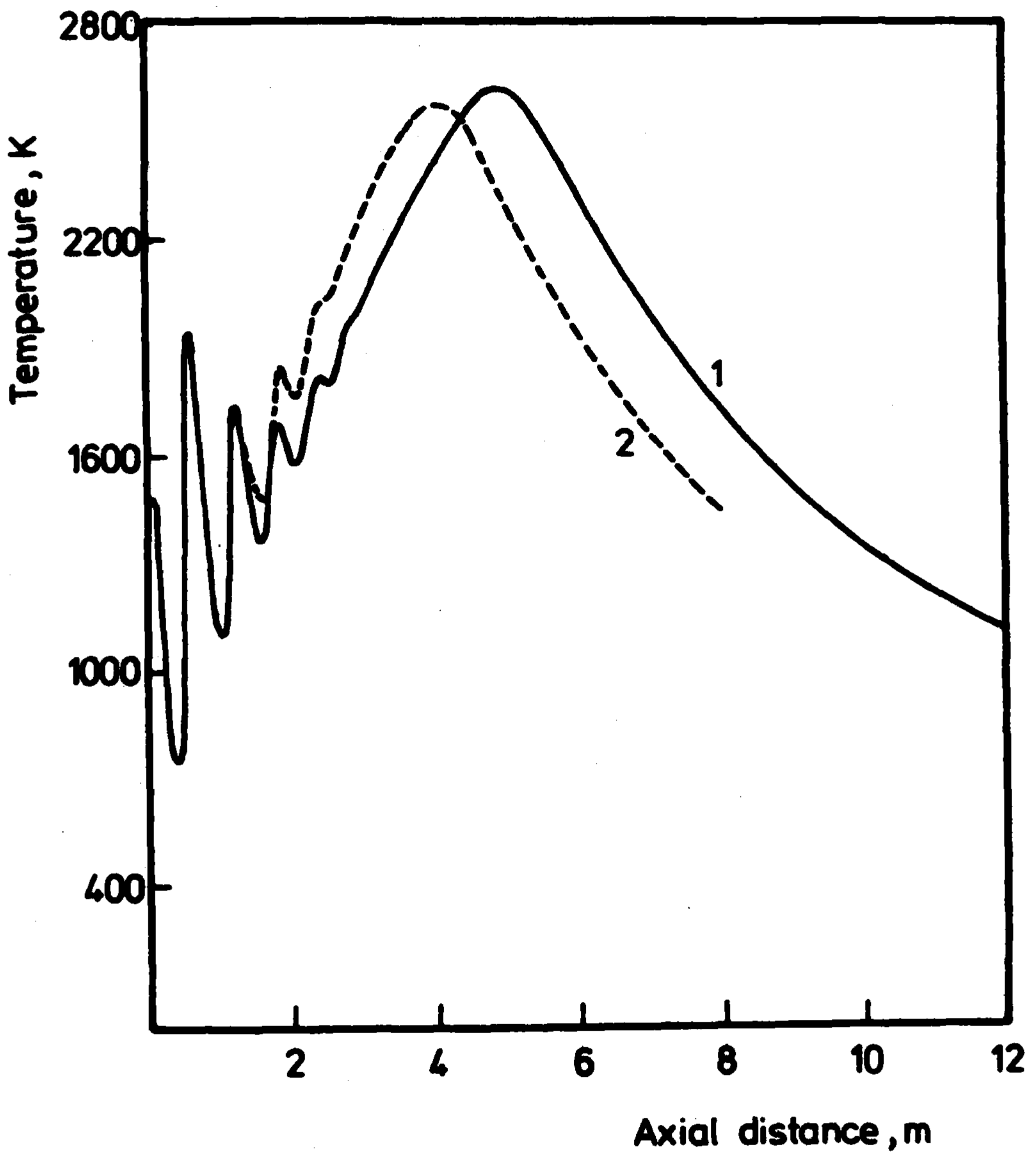

FIG. 5 AXIAL TEMPERATURE PROFILES: LINE 1, STANDARD INPUT DATA; LINE 2, $Pr_t = Sc_t = 0.7$, OTHERWISE STANDARD INPUTS.

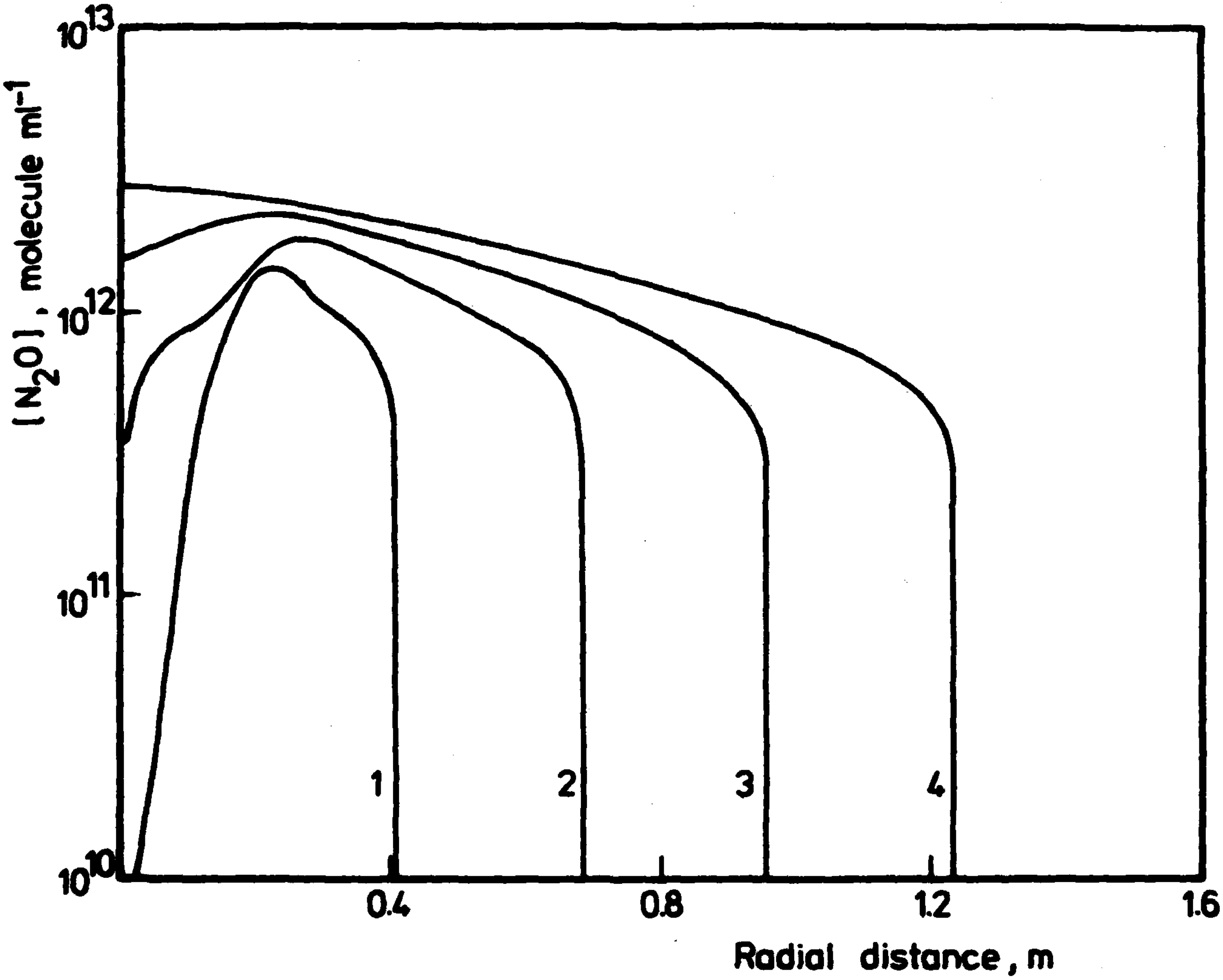

FIG. 6 RADIAL PROFILES OF $[N_2O]$ FOR $Pr_t = Sc_t = 0.7$ BUT OTHERWISE STANDARD INPUT DATA.

1, x = 2 m; 2, x = 4 m; 3, x = 6 m; 4, x = 8 m.

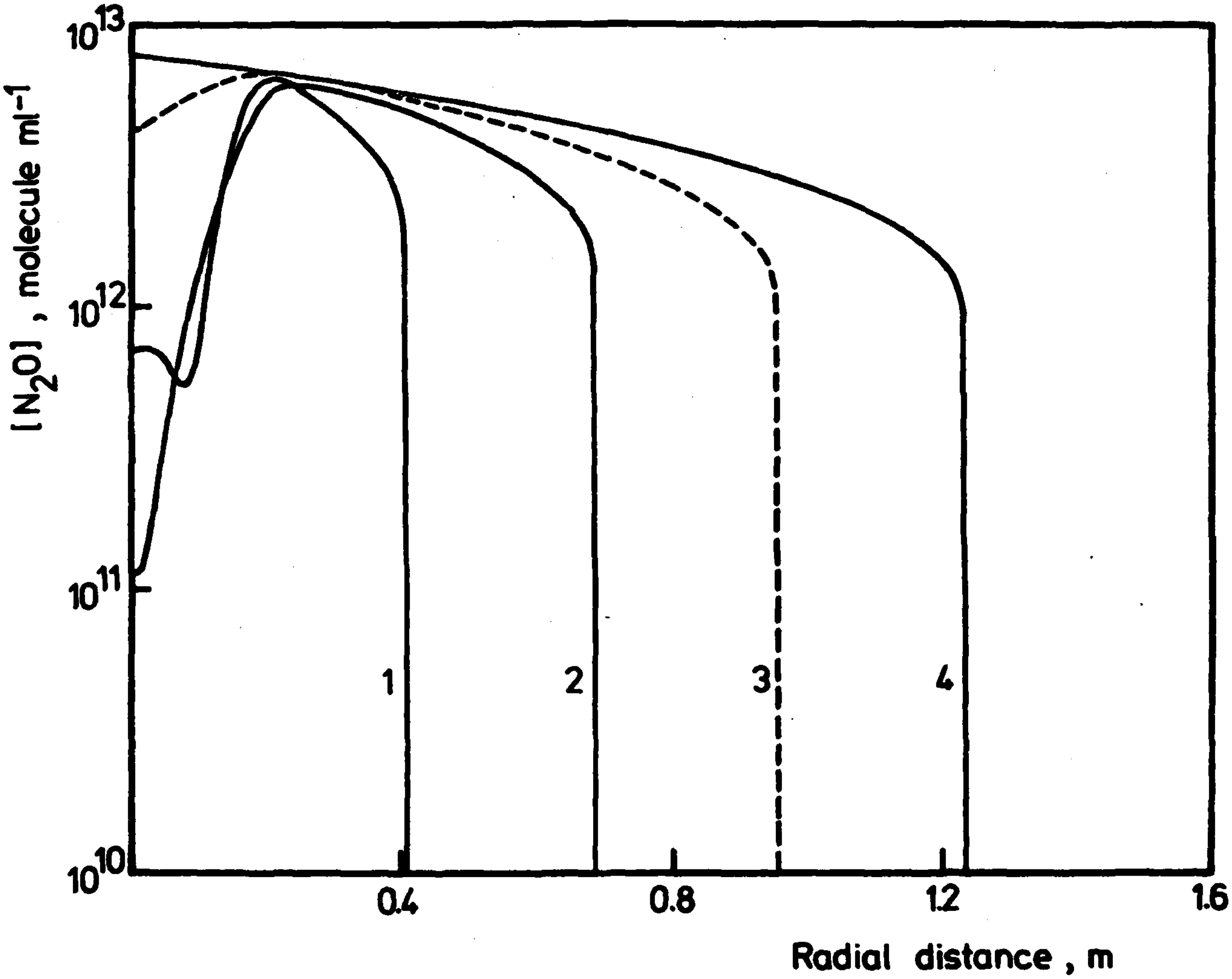

FIG. 7 RADIAL PROFILES OF $[N_2O]$ FOR $Pr_t = Sc_t = 0.7$, AND FOR ALL REACTIONS OF NITROGEN-CONTAINING SPECIES EXCEPT 26 AND 27 EXCLUDED, BUT OTHERWISE STANDARD INPUTS.

1, x = 2 m; 2, x = 4 m; 3, x = 6 m; 4, x = 8 m.

DOCUMENT CONTROL SHEET

(Notes on completion overleaf)

Overall security classification of sheet UNLIMITED .....Unclassified.....

(As far as possible this sheet should contain only unclassified information. If is is necessary to enter classified information, the box concerned must be marked to indicate the classification eg (R),(C) or (S)).

1. DRIC Reference (if known)	2. Originator's Reference	3. Agency Reference	4. Report Security Classification
	Memorandum 96		UNLIMITED Unclassified

5. Originator's Code (if known)	6. Originator (Corporate Author) Name and Location
7281500 M	Propellants, Explosives and Rocket Motor Establishment, Westcott, Aylesbury, Bucks.
5a. Sponsoring Agency's Code (if known)	6a. Sponsoring Agency (Contract Authority) Name and Location

7. Title

PRODUCTION OF NITROUS OXIDE IN A ROCKET MOTOR EXHAUST

7a. Title in Foreign Language (in the case of translations)

7b. Presented at (for conference papers). Title, place and date of conference

8. Author 1, Surname, initials	9a Author 2	9b Authors 3, 4...	10. Date	pp	ref
Jensen, D.E.			8.1980	15	9

11. Contract Number	12. Period	13. Project	14. Other References

15. Distribution statement

Unlimited

15. Descriptors (or keywords) (TEST)

Rocket exhaust; Nitrogen oxides; Combustion; Reaction kinetics.

continue on separate piece of paper if necessary

Abstract

Predictions are made of concentrations of N_2O produced within the exhaust of a double-base propellant rocket motor. Typical concentrations produced are predicted to be between 10^{12} and 10^{13} molecule ml^{-1}, some five orders of magnitude below those of CO_2 and lower than the characteristic atmospheric level of about 1.3×10^{13} molecule ml^{-1}.